Al-Khwarizmi Engineering Journal, Vol. 19, No. 4, December, (2023)
P. P. 16- 28

Al-Khwarizmi Engineering Journal

The Remediation of Congo Red-Contaminated Groundwater by using a Permeable Reactive Barrier Through Modified Waterworks Sludge MgAl-LDH

Sudad Adil Salih* **Tariq M. Naife****

*,** *Department of Chemical Engineering/ University of Baghdad/ Baghdad/ Iraq*

Corresponding Author *Email: Sudad.Saleh1607m@coeng.uobaghdad.edu.iq

**Email: tariq.mohammed@coeng.uobaghdad.edu.iq

(Received 16 May 2023; accepted 5 July 2023)

https://doi.org/10.22153/kej.2023.07.001

Abstract

This investigation aims to explore the potential of waterworks sludge (WS), low-cost byproduct of water treatment processes, as a sorbent for removing Congo Red (CR) dyes. This will be achieved by precipitating nano-sized (MgAl-LDH)-layered double hydroxide onto the surface of the sludge. The efficiency of utilizing MgAl-LDH to modify waterworks sludge (MWS) for use in permeable reactive barrier technology was confirmed through analysis with Fourier transform infrared and X-ray diffraction. The isotherm model was employed to elucidate the adsorption mechanisms involved in the process. Furthermore, the COMSOL model was utilized to establish a continuous testing model for the analysis of contaminant transport under diverse conditions. A strong correlation was indicated, with a coefficient of determination (R2) ≥ 0.97, when the model's predictions were compared to experimental values, indicating the accuracy of the model. Continuous transport exhibited earlier breakthrough points when the bed depth decreased and the initial concentration and flow rate increased.

Keywords: *Layered Double Hydroxide, Waterworks Sludge, Congo Red.*

1. Introduction

Groundwater, being one of the most abundant water sources, is often regarded as a more dependable option compared to surface water for a variety of applications [1]–[3]. The contamination of this valuable resource is a significant environmental concern, as the majority of pollutants resulting from human activities or unnatural sources can have long-lasting and detrimental effects [4]–[7]. Aromatic molecular structures present in dyes pose a considerable challenge for biodegradation into environmentally benign compounds and can have severe toxicity towards various microorganisms [8], [9]. With its anionic and acidic properties, CR can act as an antifungal therapeutic agent in various fields, such as commercial fish hatcheries and animal husbandry [10]–[12]. However, it can have adverse effects on humans, such as amyloidosis [13]; As a result, it has been banned in Europe, the United States, Canada, and other parts of the world [14]. To guarantee the safe disposal of wastewater, it is essential to eliminate CR from it. Several physical and chemical methods have been employed for this purpose, such as coagulation and flocculation, which are used for removing dyes from wastewater [15], biological degradation[14], adsorption [16], membrane filtration [17], [18], and ultra-chemical filtration [1], [19]. Although these methods are effective, they have technical limitations such as high costs, low processing capacity, and the potential for secondary pollution.

The effectiveness, simplicity, and versatility of adsorption make it widely recognized as the optimal method for the removal of CR dye. While

various adsorbents have been explored, including activated carbons [20] and natural biosorbents [21], they often fail to meet the requirements for CR dye removal due to low adsorption capacity, long diffusion times, or poor structural stability. Investigating advanced adsorbents that can efficiently capture CR dye is crucial. Permeable reactive barriers (PRBs) have demonstrated the potential to restrict and contain contaminant migration, protecting water resources. Choosing the appropriate material for PRBs is crucial, as it must be reactive and possess permeability that matches or surpasses that of the surrounding aquifer. Furthermore, innovative remediation techniques are required to treat groundwater contaminated with heavy metals and other pollutants [22]–[24].

Millions of tons of waterworks sludge (WS) are generated annually in Europe [8], [9], with the potential for a significant increase in the future. Although classified as "non-hazardous" under EU regulations, sludge disposal in sanitary landfills can result in increased costs in some countries. Conversely, in other countries, the direct discharge of sludge into rivers has caused a significant rise in surface water turbidity. This study aims to address this issue by developing a novel sorbent. The sorbent will be created by coating WS with layered double hydroxide (MWS) to efficiently remove CR dyes. The efficacy of the composite material will be assessed through two main steps: first, by determining the mechanisms involved in dye removal using XRD and FT-IR analysis, and second, by tracking the migration of the dye front through a physical column filled with the prepared sorbent and mathematically describing this movement using solute transport equations.

2. Mathematical Model

2.1 Adsorption Isotherms

The adsorbate concentration in the state of the liquid and its concentration on the adsorbent surface at a particular temperature are related by the isotherm model, which is frequently utilized to explain adsorption. The equilibrium concentration of the adsorbate in solution (Ce) (mg/L) is shown against the amount of adsorbate per unit mass of adsorb (qe) (mg/g). This number is typically uniformed by the quantity of adsorbent to make comparisons with various substances simple. Adsorbent concentration is not increasing proportionally to the amount of adsorbed material per unit mass of adsorbent.This research utilized various adsorption isotherm models, and a brief overview of these models is presented below. A favorable isotherm is one that is upwardly convex, indicating that the solid content remains relatively high even at low concentrations in the liquid. The first non-linear isotherm was introduced by Freundlich and Kuster.In order to characterize the dispersion of chemicals between the two states of matter, Irving Langmuir developed a non-linear model in 1916. [25]:

$$q_e = K_f C_e^{1/n} \quad \dots (1)$$

$$q_e = \frac{q_m b C_e}{1+bC_e} \quad \dots (2)$$

Where Kf $(mg/g)(L/mg)^{1/n}$ and n are Freundlich constants related to adsorption capacity and adsorption intensity, respectively. qm (mg/g) and b (L/mg) are used to describe the maximum adsorption capacity and energy of adsorption, respectively.

2.2 Modeling of dissolved contaminants

Three fundamental processes govern the transportation of contaminants in the subsurface environment, as stated by [26]: molecular diffusion, advection, and mechanical dispersion.

1. Molecular diffusion: Fick's first law defines the diffusion of solutes, where the movement of solutes is from high concentration regions to low concentration regions. The quantity of transported solute is proportional to its concentration and can be mathematically expressed in one dimension [27].

$$F = -D_d \left(\frac{dC}{dx}\right) \quad \dots(3)$$

where F refers to solute mass flow per unit area (kg /(m^2 s)), Dd for diffusion coefficient (m^2/s), C for solute concentration (mg/L), and dC/dx for concentration gradient per unit length.

Fick's second law [28] should always be applied in situations where concentration may evolve over time:

$$\frac{\partial C}{\partial t} = D_d \frac{\partial^2 C}{\partial x^2} \quad \dots (4)$$

Diffusion in porous media is slower than in water because the ions must travel along longer paths as they pass through mineral-solid grains. Furthermore, diffusion can only occur through pore holes. To address this, an efficient diffusion coefficient can be used [27]:

$$D^* = \tau D_d \quad \dots (5)$$

where τ is a tortuosity factor and its values ranged from 0.01 to 0.5 [27].

2. Advection: is the process that moves contaminants through the groundwater. The rate of

advection and the flow rate of groundwater are the same. The Darcy velocity (V) (m/s) is the same as the actual velocity (Va) (m/s), which is related to porosity (n). The advictive flux (Fa) is calculated as follows [27]:

$$F_a = V_a C = \frac{V}{n} C \quad \dots (6)$$

Mechanical dispersion: occurs when water containing the chemical(s) flows around the soil grains in the aquifer, resulting in mixing. Molecules of water actually move more quickly and slower than the average linear velocity due to three factors: fluid moves faster in the centre of pores than at the edges, some molecules follow longer discrete paths, and several voids are larger than others, allowing faster flow. Mechanical mixing appears to happen along the flow path because water molecules don't move at the same velocity. This mixing (or dispersion) can dilute the solute at the propagating edge of flow through longitudinal and transverse dispersions.

Separating the mechanisms of mechanical dispersion and diffusion in swirling groundwater is unfeasible. They're categorized together and referred to as "hydrodynamic dispersion" as follows [27]:

$$D_L = \alpha_L V_L + D^* \quad \dots (7)$$

Where L and T stand for longitudinal and transverse dispersivities, respectively, the coefficients of longitudinal and transverse hydrodynamic dispersions are denoted as DL and DT(m^2/s).

In the subsurface environment, chemical reactions can lead to changes in a compound's properties, conversion into a different form, or reaction with other chemicals. Isotherms, which consider how the concentrations of the reactants impact the reaction rate, are widely used to explain these processes [29]. Sorption is the most valuable chemical reaction in the subsurface environment for the transport of inorganic and organic impurities. Sorption represents the solute adhering to the surfaces of solid particles, causing it to take longer to arrive.

The flow of an individual dissolved component into and out of a MWS elemental control volume, F, is taken into account by the mass conservation equation, which is provided by:

$$-\left(\frac{\partial F}{\partial x} + \frac{\partial F}{\partial y} + \frac{\partial F}{\partial z}\right) \mp r = \frac{\partial m}{\partial t} = \frac{\partial (nC)}{\partial t} \quad \dots (8)$$

where r is the reaction term, which may be either a (+) source or a (-) sink for the solute and m is the mass per unit volume.

Eq. 9 can be written as follows after substitution of advective flux (=V_x n C) and dispersive flux (=-n$D_x\frac{\partial C}{\partial x}$): $-\left[\frac{\partial}{\partial x}\left(V_x nC - nD_x\frac{\partial C}{\partial x}\right)\right] - \left[\frac{\partial}{\partial y}\left(V_y nC - nD_y\frac{\partial C}{\partial y}\right)\right] - \left[\frac{\partial}{\partial z}\left(V_z nC - nD_z\frac{\partial C}{\partial z}\right)\right] \pm r = \frac{\partial (nC)}{\partial t}$ …(9)

By considering a steady flow velocity, dispersion coefficient, and porosity, the well-known advection-dispersion formula could potentially be utilized to determine the 1 D mass transport of a solute in the saturated zone [27].

$$D_z\frac{\partial^2 C}{\partial z^2} - V_z\frac{\partial C}{\partial z} \pm \frac{r}{n} = \frac{\partial C}{\partial t} \quad \dots (10)$$

The specific form of Eq. 11 is determined by the outcome term's shape. Perhaps the most frequent mass transfer process what occurs in the transportation of mass is adsorption, which tends to be the main mechanism for the operation of PRB_S The following equation can be used to determine r's value [30]:

$$r = \rho_b\frac{\partial q}{\partial t} \quad \dots (11)$$

Eq.11 can be integrated with Eq.15 to obtain the following equation [31]:

$$D_z\frac{\partial^2 C}{\partial z^2} - V_z\frac{\partial C}{\partial z} = \frac{\partial C}{\partial t} + \frac{\rho_b}{n}\frac{\partial (q)}{\partial t} \quad \dots (12)$$

Where ρ_b is the dry bulk density and q is the solute concentration sorbed on the sorbent. The Langmuir or Freundlich isotherm model can be used to describe the values of q (mg/g) as a function of concentration. Eq.12 can be rewritten as follows:

$$D_z\frac{\partial^2 C}{\partial z^2} - V_z\frac{\partial C}{\partial z} = R\frac{\partial C}{\partial t} \quad \dots (13)$$

The retardation factor (R) is used to describe the decrease in solute transport in relation to advection. The advection-dispersion equation (ADE) can be used to determine the one-dimensional mass transport of solute in the saturated zone, assuming constant flow velocity, dispersion coefficient, and porosity. Boundary and initial conditions that describe the physical state of the process must be provided to fully define the equation. The boundary conditions represent the geometry of the flow domain and the values of the dependent variable or its derivative [32].

Numerical models for solute transport are useful in designing remedial programs as they provide valuable information about mass transport. These models divide the flow region into finite elements or grid cells, with each element representing a bounded portion of the flow region. The solution obtained for each element depends on adjacent segments as well as a set of auxiliary conditions that describe the domain geometry, variables, boundary conditions, and initial values. Numerous numerical techniques, including the boundary element technique,the finite difference method, and finite element procedure, are currently being produced. Groundwater transport formulas are discretized utilizing the finite element method

(FEM), which produces a set of algebraic differential equations. Mathematical techniques are able to be utilized to solve these types of issues [33]. In the current work, a partial-differential equation (PDE) governing the transient transport of CR in the saturated zone (Eq. 13) has been calculated using the finite element method followed by a solution with COMSOL Multiphysics 3.5a. The PDE was solved using the "Earth Science module" of the software in the "saturated solute transport" option.

2.3 Coefficient of dispersion

To measure the coefficient of hydraulic conductivity in the direction of flow, a tracer experiment was conducted on a column packed with 0.5 m of dry reactive material. Water was injected in an upward direction to avoid entrapping air in the voids between solid grains. For the tracer experiment, one gram of NaCl was dissolved in deionized water (1 L), which was subsequently injected at flow rates between 5 and 20 mL/min into the packed column. NaCl was selected because of its accessibility, safety, and simplicity of detection. Electrical conductivities corresponding to NaCl concentrations were measured at certain time intervals during the experiment, and these values were used to determine the coefficient of dispersion in the longitudinal direction (DL) using the following equation [34]:

$$D_L = \frac{1}{8}\left[\frac{(z_o - Vt_{0.16})}{(t_{0.16})^{0.5}} - \frac{(z_o - Vt_{0.84})}{(t_{0.84})^{0.5}}\right]^2 \quad \ldots(14)$$

Here, zo represents the bed depth (0.5 m), V is the velocity in the voids, and t0.84 and t0.16 are times corresponding to 84% and 16% of C/Co, respectively.

3. Experimental Work

3.1 Materials and Methods

The research concentrated on CR dyes that were procured from the HIMEDIA company in India. To prepare the initial dye solution, a specific amount of CR was mixed with distilled water (1 liter), resulting in a solution with an CR concentration (1000 mg/L). A dilution was employed to obtain various concentrations of the dye in the water samples. To adjust the pH of the samples, drops of HCl or NaOH(1 M) were added. The sludge was obtained from the Water Treatment (AL-Weihdaa) in Baghdad, Iraq. During treatment, alum salts were added to the sedimentation tank. The sludge was dried for several days and then ground into a fine powder. In addition to characterization using FTIR, the hydraulic conductivity of the sludge was also measured and found to be low at 0.0245 cm/s. This low hydraulic conductivity may result in blockages during continuous flow in a PRB. Coarse sand was employed in various proportions along with the sludge to enhance hydraulic conductivity, aiming to overcome the inherent low hydraulic conductivity of the sludge. The sand used in the experiment had a particle size ranging between 1.7 and 3.15 mm.

3.2 Modification of WS

To create an affordable sorbent with enhanced reactivity, WS was employed as a matrix for immobilization, and its surface was subsequently coated with nanoparticles of layered double hydroxide (Mg/Al-LDH). The procedure involved mixing 25 mL each of Magnesium nitrate hexahydrate (0.1 M) and Aluminium nitrate nonahydrate (0.05 M) and adjusting the pH to 11 using 1 M NH4OH. WS was added to synthetic new functional groups, and the resulting sorbent was washed with water until the pH reached 6.5-7. Through the application of (Mg/Al)-layered double hydroxide (LDH) nanoparticles, the WS underwent a transformation, resulting in the formation of modified WS (MWS) with a coated surface. XRD and FT-IR were utilized to analyze the coating method and to find any functional groups in the MWS. The efficacy of the MWS in removing CR dyes from contaminated water was evaluated through analysis of the dye concentration, with the experimental methods and setup described in detail to ensure accurate measurements.

3.3 Characterization

XRD analysis was conducted using the D/MAX 2500 V/PC from Rigaku, Japan, to identify the coated and virgin WS crystal structures. FT-IR analysis was conducted to identify the functional groups that improve the sorption capacity of the prepared sorbent. The analysis was carried out using a Bruker Tensor 27 spectrophotometer with the KBr pellet technique, and the spectra were recorded in the range of 4000 to 400 cm^{-1}.

3.4 Continuous Study

The reactivity of the filler material in removing CR from contaminated water was evaluated using a number of column tests. The sorbent's efficiency was evaluated based on its ability to eliminate

pollutants. A column experiment was performed to evaluate the reactivity and hydraulic performance of MWS. The column was 2 and 50 cm in diameter and height, respectively, with sampling ports (P1 to P6) located every 5 cm from the bottom, covered by plastic valves. In order to prevent the trapping of air between the particles, the MWS was carefully introduced into the column, and distilled water was slowly introduced from the bottom using a peristaltic pump. The tests performed in the column lasted 90 hours and throughout that time the amount of CR in the effluent water was continuously monitored. The samples of water were promptly analyzed with the help of a UV-spectrophotometer [4].

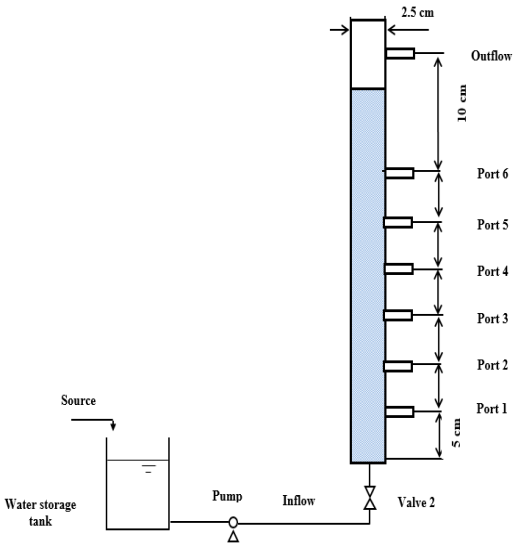

Fig. 1. Details of Continuous Study.

4. Results and Discussion

4.1 Adsorbent characteristics

The XRD spectrum in Fig. 2 shows the crystal structure of MWS. In order to compare the crystalline structures of the composite sorbent and sludge, XRD analysis was conducted on both materials, and their profiles are depicted in Fig. 2 alongside the Joint Committee on Powder Diffraction Standards (JCPDSs). The analysis indicated that iron oxide, calcite, and silica oxide are the primary components of WS. However, the MWS XRD pattern showed a new peak at 18.01, 26.6, and 34.1°, suggesting the existence of Mg/Fe crystals. The findings indicate that the MWS sorbent's synthesis was successful [35]–[40]. Fig. 2 displays the infrared spectra of WS, MWS, CR dye, and the sorbent after adsorption within the 400 to 4000 cm-1 range. The significant peak at 3491 cm1 represents the stretching vibration of inter-lamellar water-linked -OH groups, O-H groups of adjacent layers, and physically adsorbed water. Bound H2O has been detected demonstrated by the shift at 1648 cm-1.

The relationship with CR is confirmed by the Raman spectra of -OH at 3491 cm-1. O-M-O and M-O (where M is a metal) vibrations in the lattice frequently correspond to the peak that is nearest to 531 cm-1. The effective modification of WS is further demonstrated by the identification of a new peak at 1348 cm1 in the MWS compared with WS, that corresponds to the CO32's in-of-plane vibration band with an asymmetric stretch absorption band. After CR adsorption, two separate peak shapes near 1080 and 1159 cm-1, that relate to the vibrations of the S=O and aromatic ring structures of the CR, accordingly, were observed. These results indicate that coated WS surfaces are successful in adsorbing CR.

4.2 Sorption Isotherm Models

When equilibrium occurs in the procedure of adsorption, the adsorption isotherm can potentially be utilized to determine how CR are distributed throughout the MWS and water phases. Moreover, this isotherm can also be used to find out the highest amount of adsorbate that can be adsorbed and the attraction of the adsorbent towards the adsorbate [41], [42]. In the present study, two commonly utilized sorption isotherm models—Langmuir and Freundlich—were utilized to correlate with the experimental data from research on adsorption on MWS. The experiments were conducted under optimal conditions with selected contaminants at varying concentrations. During the preparation process, mixing speed and time were critical factors that influenced the hydraulic conductivity of the sorbent and its suitability for continuous use. The appropriate isotherm model was utilized to determine the retardation factor in the advection-dispersion formula that clarifies the movement of CR along PRB. For nonlinear regression calculations, the Freundlich and Langmuir isotherm models were utilized, and the parameter values obtained from these models are displayed in Table 2. Depending on the R2 and SSE numbers, it was found that the Langmuir model was more appropriate compared to the Freundlich model.

The Langmuir constants have been determined to be 0.08 L/mg. The match between the experimental results and the sorption equilibrium models can be observed in Fig. 3. The highest

adsorption capacity of MWS for CR was found to be 23.57 mg/g. This finding indicates higher adsorption capacity due to CR bind with the MSW more effectively.

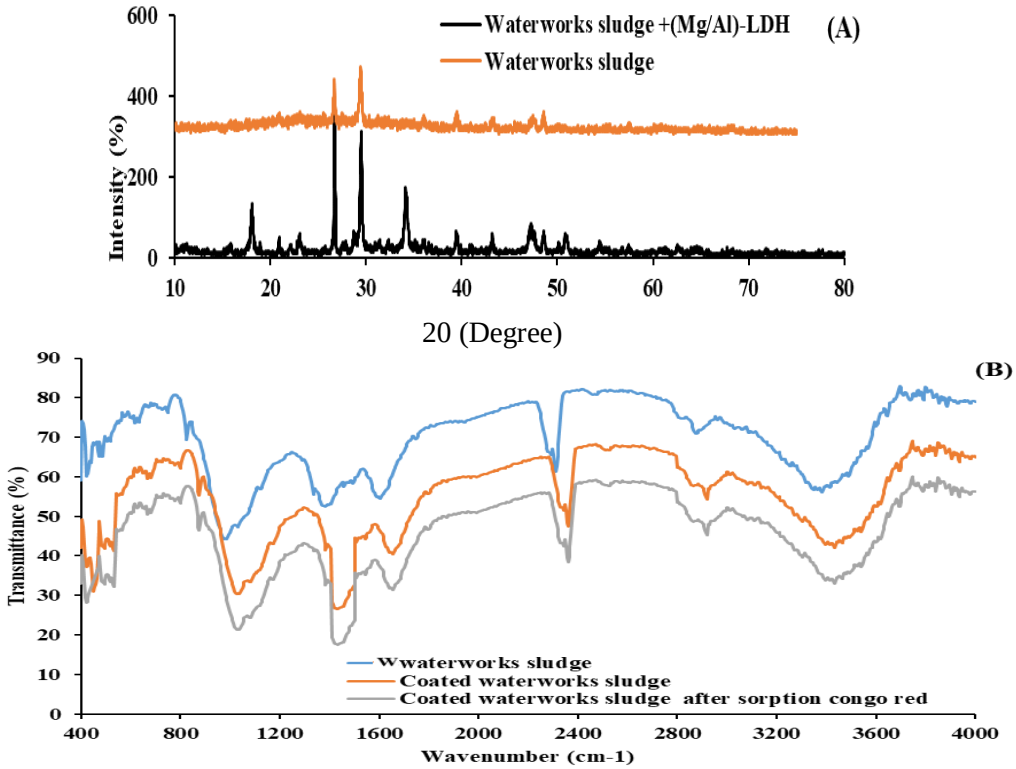

Fig. 2. X-ray diffraction (A) and FT-IR analysis pattern (B) for crystalline structure of WS, MWS, CR, and sorbent after adsorption.

4.3 Longitudinal Dispersion Coefficient

In columns packed with a 1:15 proportion of sludge and sand, the aim of the present investigation was to explore the relationship between average pore velocity (V) and longitudinal dispersion coefficient (DL). To attain laminar flow conditions, flow rates were adjusted to 5, 10, 15, and 20 mL/min, ensuring that Reynolds numbers (Re) were maintained below 1-10. Based on the data obtained from the experiment, as shown in Fig. 3, it was observed that there exists a linear association between DL and V.

$$D_L = 13.953V + 0.046 \quad \ldots (15)$$

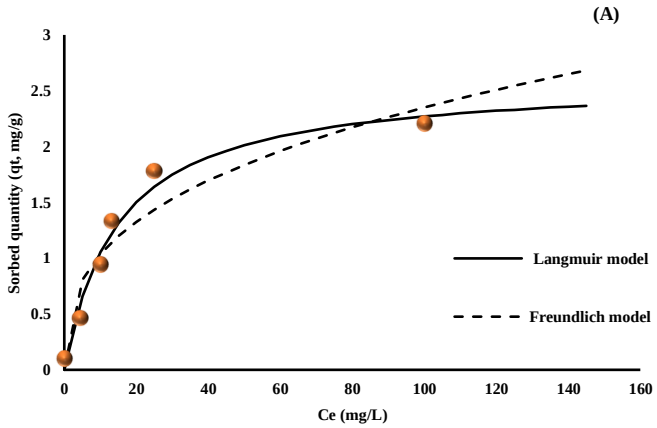

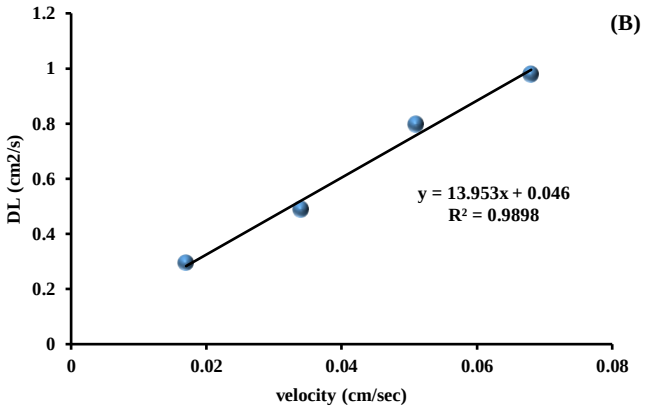

Fig. 3. The experimental results of MWS and specifically the sand ratio (1:15), were compared with various isotherm models (A), and the longitudinal dispersion coefficient (B).

The relationship between DL and V found in this study agrees with the relationship expressed in Equation 16. In this equation, the
The proportionality factor αL links dispersion and velocity in the longitudinal direction and has a dimension of length. This relationship is additionally influenced by the tortuosity (τ), which evaluates the impact of the water transition across a porous mediam which is influenced by the porosity of the medium (n).

$$\tau = n^{m-1} \quad \dots (16)$$

The value of the parameter tortuosity (τ), that is affected by the material's porosity (n), is essential in explaining how the shape of the flow route influences the movement of water in a porous medium. Eq. 16, where the constant value of m relies on the medium's aggregation phase, illustrates the connection between and n. In a laboratory experiment, Archie (1942) found a value of 1.3 for unpacked sand, 1.8-2 for consolidated sandstone, and 1.3-2 for partly established sand. Using the similarity between Eq. 15 and Eq. 16, the longitudinal dispersivity (αL) can be calculated for the PRB medium (Sludge:sand (1:15)).

4.4 Column Tests

A permeable reactive barrier (PRB) made of a sludge-sand (1:15) mixture was evaluated for its ability to remove CR contaminants from aqueous solutions while maintaining an acceptable hydraulic conductivity coefficient. The study utilized a column setup (Fig. 1) and considered the rate of flow, concentration of chemical species, and bed depth. The study observed the normalized concentration (C/Co) of the adopted contaminants with time at ports P1-P6 for a duration of up to 100 hours, as well as the variation in hydraulic conductivity coefficient (K) during the operation time. The advection-dispersion-sorption equation, which was numerically solved using the finite element method and the COMSOL program, was used to theoretically approximate the experimental breakthrough curves.

Table 2,
Isotherm model constants with statistical analysis for sorption CR.

Adsorbent Model	Parameter	MWS : sand (1:15)
Langmuir	q_{nax}	2.604
	b	0.068
	R^2	0.976
	SSE	0.075
Freundlich	k_f	0.456
	N	2.810
	R^2	0.909
	SSE	0.298

Figure 4 depicts the outcomes of evaluating the normalized concentrations of CR at effluent ports P1 to P6 for up to 100 hours at a flow rate of 5 mL/min.

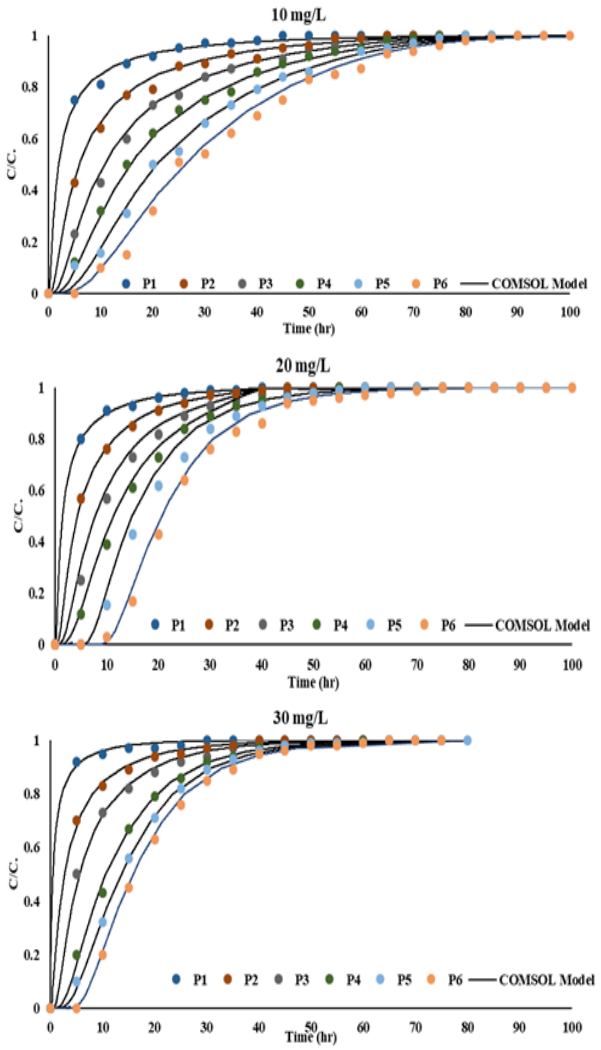

Fig. 4. Relationship between experimental findings and COMSOL results for the normalized concentration of CR under the influence of the initial concentration at various ports.

The research discovered that the permeable reactive barrier (PRB) impedes the spread of CR, and the concentration gradient has the potential to impact the saturation rate of the bed. The curve's shape is less prominent at lower influent concentrations due to sluggish sorption, while raising the influent concentration causes a steeper slope, leading to saturation of the sorbent in a shorter period. A low concentration gradient prolongs the propagation of chemical species through the pores, extending the time to reach saturation.

The investigation revealed that the breakthrough time (tb) of 5% and saturation time (ts) of 90% rise with decreasing normalized concentration (C/Co), affecting the adsorbed quantities of the contaminant at breakthrough and saturation points within the bed. With higher influent concentrations, the saturation of the adsorption process occurs more rapidly, leading to a decrease in breakthrough time. This phenomenon can be attributed to the presence of a larger concentration gradient, which intensifies the driving force for mass transfer of contaminant molecules. Consequently, the adsorption sites become covered more quickly. Additionally, the study observed that the adsorption capacity did not exhibit a proportional increase with rising influent concentration [43]–[45].

The purpose of the study was to examine how varying water flow rates affect the ability of a sorbent barrier to adsorb CR. By accounting for normalized concentrations at various points in the column using a variety of flow rates (5, 10, and 15 mL/min) and a fixed CR concentration of 10 mg/L, breakthrough curves were obtained. The findings demonstrated that with an increase in flow rate, the breakthrough time decreased and the curves exhibited a steeper slope. These observations suggested that the contaminated solution had not reached equilibrium within the column due to the reduced residence time caused by the higher flow rate. The faster flow rate also improved solute transport and increased sorption by creating a concentration gradient at the interface between the liquid and sorbent. However, the higher flow rate resulted in reduced solute adhesion to the sorbent and lower sorption efficiency, which could cause desorption of some adsorbed contaminant molecules, leading to an earlier breakthrough time. As a result, a lower flow rate was found to be more effective in adsorbing contaminants in the fixed bed due to its higher adsorption capacity. The study concluded that optimizing the water flow rate is critical for achieving maximum sorption efficiency in fixed bed adsorption systems [44], [46]–[48].

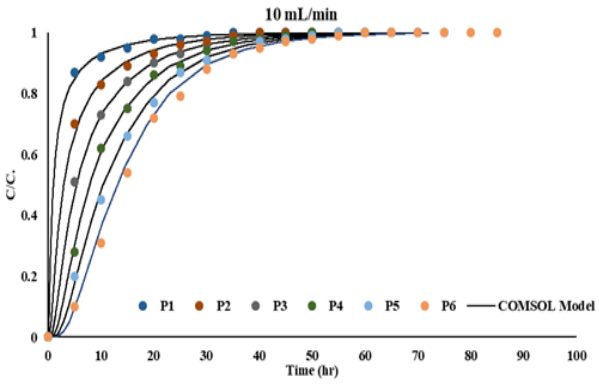

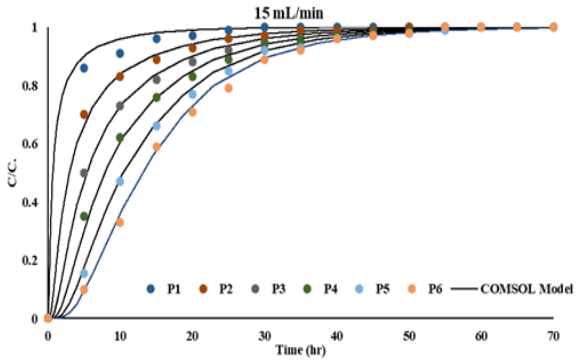

Fig. 5. Relationship of experimental data and COMSOL results indicates a normalized concentration of CR with the impact of flow rate at various ports .

In order to examine the impact of bed depth on sorption capacity, Figures 4 and 5 were used. The findings demonstrated the same influent concentration and flow rate, adding more sorbent increased sorption capacity. The usual S-shaped breakthrough curves for CR adsorption indicate that as the bed depth increased the breakthrough time decreased and the effluent quantity increased. In continuous adsorption experiments, the sorbent reached an exhaust time at which it could no longer adsorb solute molecules, represented by a C/Co of 0.9. The exhaust time was found to increase with increasing bed height, indicating that higher bed depths provided more active sites for adsorption. More time was provided for the adsorbate molecules to diffuse into the pores of the adsorbent particles, resulting in more contaminant molecules being adsorbed. As a result, the effluent volume increased with increasing exhaust time due to the higher bed depth. However, the adsorption capacity for contaminants decreased with increasing bed height due to two reasons: firstly, at higher bed heights, all binding sites become inaccessible to adsorbate molecules because of the overlap of active sites, resulting in some particles being inadequately utilized. Secondly, lower bed depths were found to be more favorable for contaminant adsorption capacity, which is consistent with the findings of previous studies. Therefore, it is crucial to use the entire capacity of an adsorbent for it to be effectively utilized in industrial applications [48].

4.5 Numerical Modelling

The study employed COMSOL Multiphysics 3.5a (2008) software to solve the advection-dispersion equation. The software incorporates several modules, such as Earth Science, Solute Transport, Saturated Porous Media, and Transient Analysis. Simulation processes were established by inputting system dimensions and attributes, including boundary and initial conditions, as specified in Table 3. One-dimensional measurements of column bed parameters and constants were used to characterize solute transport. The comparison between simulated results of contaminant transport and experimental measurements taken at different time intervals for a specific influent concentration and flow rate, revealed a high level of consistency. The coefficient of determination (R2) exceeded 0.97, indicating strong agreement between the model predictions and experimental data.

Table 3.
Adopted data used for simulating CR transport in columns.

Item	Parameter	Value
Aquifer characteristics	Aquifer bed depth (cm)	50
	Porosity of aquifer (n_A)	0.38
	Longitudinal dispersivity (α_L, cm)	13.953
	Bulk density (g/cm^3)	1.677
Initial condition	Initial concentration (mg/l)	zero

5. Conclusions

This study aimed to investigate utilizing WS as a low-cost byproduct for water treatment procedures and decontaminating groundwater from CR. To achieve this goal, the WS sludge was modified using MgAl-LDH-sand to create a permeable reactive barrier. The tests demonstrated successful remediation of the CR. Langmuir modeling revealed that the modified sludge had exceptional sorption capacity, with a maximum adsorption capacity of 23.575mg/g. To accurately predict the behavior of different CR concentrations and bed depths, a mathematical model was utilized. The model was solved using the COMSOL software, and the accuracy of the results was confirmed with an R2 value greater than or equal to 0.97. These findings suggest that modified WS has the potential to be a cost-effective and efficient solution for treating groundwater contaminated with CR dye.

Acknowledgements

We would like to express our gratitude for the technical assistance and support provided by the Chemical Engineering Department at the University of Baghdad, Iraq, during the course of this research.

References

[1] A. A. H. Faisal, L. A. Naji, A. A. Chaudhary, and B. Saleh, "Removal of ammoniacal nitrogen from contaminated groundwater using waste foundry sand in the permeable reactive barrier," *Desalin. WATER Treat.*, vol. 230, pp. 227–239, 2021.

[2] A. A. H. Faisal, Z. A. Al-Ridah, L. A. Naji, M. Naushad, and H. A. El-Serehy, "Waste Foundry Sand as Permeable and Low Permeable Barrier for Restriction of the Propagation of Lead and Nickel Ions in Groundwater," *J. Chem.*, vol. 2020, pp. 1–13, Jul. 2020.

[3] D. N. Ahmed, A. A. H. Faisal, S. H. Jassam, L. A. Naji, and M. Naushad, "Kinetic Model for pH Variation Resulted from Interaction of Aqueous Solution Contaminated with Nickel Ions and Cement Kiln Dust," *J. Chem.*, vol. 2020, pp. 1–11, Apr. 2020.

[4] A. A. H. Faisal, H. K. Jasim, L. A. Naji, M. Naushad, and T. Ahamad, "Cement kiln dust-sand permeable reactive barrier for remediation of groundwater contaminated with dissolved benzene," *Sep. Sci. Technol.*, pp. 1–14, Apr. 2020.

[5] L. A. Naji, A. A. H. Faisal, H. M. Rashid, M. Naushad, and T. Ahamad, "Environmental remediation of synthetic leachate produced from sanitary landfills using low-cost composite sorbent," *Environ. Technol. Innov.*, vol. 175, p. 100680, Feb. 2020.

[6] L. A. Naji, S. H. Jassam, M. J. Yaseen, A. A. H. Faisal, and N. Al-Ansari, "Modification of Langmuir model for simulating initial pH and temperature effects on sorption process," *Sep. Sci. Technol.*, vol. 55, no. 15, pp. 2729–2736, Aug. 2020.

[7] J. Z. Dhamin and N. S. Majeed, "Removal of heavy metal ions from wastewater using bulk liquid membrane technique enhanced by electrical potential," 2022, p. 020112.

[8] S. Sonal, A. Singh, and B. K. Mishra, "Decolorization of reactive dye Remazol Brilliant Blue R by zirconium oxychloride as a novel coagulant: optimization through response surface methodology," *Water Sci. Technol.*, vol. 78, no. 2, pp. 379–389, Aug. 2018.

[9] M. H. Rashid and A. H. A. Faisal, "Removal Of Dissolved Cadmium Ions from Contaminated Wastewater using Raw Scrap Zero-Valent Iron And Zero Valent Aluminum as Locally Available and Inexpensive Sorbent Wastes," *Iraqi J. Chem. Pet. Eng.*, vol. 19, no. 4, pp. 39–45, 2018.

[10] K. Sahoo, S. K. Paikra, M. Mishra, and H. Sahoo, "Amine functionalized magnetic iron oxide nanoparticles: Synthesis, antibacterial activity and rapid removal of Congo red dye," *J. Mol. Liq.*, vol. 282, pp. 428–440, May 2019.

[11] N. S. Majeed, "Inverse fluidized bed for chromium ions removal from wastewater and produced water using peanut shells as adsorbent," in *2017 International Conference on Environmental Impacts of the Oil and Gas Industries: Kurdistan Region of Iraq as a Case Study (EIOGI)*, 2017, pp. 9–14.

[12] Bassim Hameed Graimed and Z. T. A. Ali, "Thermodynamic and Kinetic Study of the Adsorption of Pb (II) from Aqueous Solution Using Bentonite and Activated Carbon," *Al-Khwarizmi Eng. J.*, vol. 9, pp. 48–56, 2013.

[13] P. Frid, S. V. Anisimov, and N. Popovic, "Congo Red and protein aggregation in neurodegenerative diseases," Brain Res Rev, vol. 53, no. 1, pp. 135–160, 2007.

[14] R. Gopinathan, J. Kanhere, and J. Banerjee, "Effect of malachite green toxicity on non target soil organisms," Chemosphere, vol. 120, pp. 637–644, Feb. 2015.

[15] J. Duan et al., "Synthesis of a novel flocculant on the basis of crosslinked Konjac glucomannan-graft-polyacrylamide-co-sodium xanthate and its application in removal of Cu2+ ion," Carbohydr. Polym., vol. 80, no. 2, pp. 436–441, Apr. 2010.

[16] M. Naushad, T. Ahamad, B. M. Al-Maswari, A. Abdullah Alqadami, and S. M. Alshehri, "Nickel ferrite bearing nitrogen-doped mesoporous carbon as efficient adsorbent for the removal of highly toxic metal ion from aqueous medium," Chem. Eng. J., vol. 330, pp. 1351–1360, Dec. 2017.

[17] A. Gürses, A. Hassani, M. Kıranşan, Ö. Açışlı, and S. Karaca, "Removal of methylene blue from aqueous solution using by untreated lignite as potential low-cost adsorbent: Kinetic, thermodynamic and equilibrium approach," *J. Water Process Eng.*, vol. 2, pp. 10–21, 2014.

[18] M. W. Khalid and S. D. Salman, "Adsorption of Heavy Metals from Aqueous Solution onto Sawdust Activated Carbon," *Al-Khwarizmi Eng. J.*, vol. 15, pp. 60–69, 2019.

[19] C. Allègre, P. Moulin, M. Maisseu, and F. Charbit, "Treatment and reuse of reactive dyeing effluents," *J. Memb. Sci.*, vol. 269, no. 1–2, pp. 15–34, Feb. 2006.

[20] A. Sharma, Z. M. Siddiqui, S. Dhar, P. Mehta, and D. Pathania, "Adsorptive removal of congo red dye (CR) from aqueous solution by Cornulaca monacantha stem and biomass-based activated carbon: isotherm, kinetics and thermodynamics," *Sep. Sci. Technol.*, vol. 54, no. 6, pp. 916–929, Apr. 2019.

[21] S. Husien, A. Labena, E. F. El-Belely, H. M. Mahmoud, and A. S. Hamouda, "Adsorption studies of hexavalent chromium [Cr (VI)] on micro-scale biomass of Sargassum dentifolium, Seaweed," *J. Environ. Chem. Eng.*, vol. 7, no. 6, p. 103444, Dec. 2019.

[22] U.-J. Kim, S. Kimura, and M. Wada, "Highly enhanced adsorption of Congo red onto dialdehyde cellulose-crosslinked cellulose-chitosan foam," *Carbohydr. Polym.*, vol. 214, pp. 294–302, Jun. 2019.

[23] S. Sultana *et al.*, "Adsorption of crystal violet dye by coconut husk powder: Isotherm, kinetics and thermodynamics perspectives," *Environ. Nanotechnology, Monit. Manag.*, vol. 17, p. 100651, May 2022.

[24] N. Saad, Z. T. Abd Ali, L. A. Naji, A. A. A. H. Faisal, and N. Al-Ansari, "Development of Bi-Langmuir model on the sorption of cadmium onto waste foundry sand: Effects of initial pH and temperature," *Environ. Eng. Res.*, vol. 25, no. 5, pp. 677–684, Sep. 2019.

[25] S. Lucas, M. J. Cocero, C. Zetzl, and G. Brunner, "Adsorption isotherms for ethylacetate and furfural on activated carbon from supercritical carbon dioxide," *Fluid Phase Equilib.*, 2004.

[26] L. Elango, *numerical simulation groundwater flow and solute transport.*, Allied Pub. 2005.

[27] S. Piazza, E. J. M. Blokker, G. Freni, V. Puleo, and M. Sambito, "Impact of diffusion and dispersion of contaminants in water distribution networks modelling and monitoring," *Water Supply*, vol. 20, no. 1, pp. 46–58, Feb. 2020.

[28] C. W. Fetter, *Contaminant hydrogeology*, 2nd ed. Prentice-Hall, New Jersey, 1999.

[29] D. W. Blowes *et al.*, "In situ permeable reactive barrier for the treatment of hexavalent chromium and trichloroethylene in ground water," Washington, D.C., 1999.

[30] A. A. H. Faisal, M. B. Abdul-Kareem, A. K. Mohammed, M. Naushad, A. A. Ghfar, and T. Ahamad, "Humic acid coated sand as a novel sorbent in permeable reactive barrier for environmental remediation of groundwater polluted with copper and cadmium ions," *J. Water Process Eng.*, vol. 36, no. April, p. 101373, Aug. 2020.

[31] Z. An, K. Grala, A. Panchal, and K. Trivedi, "Investigating graphene oxide permeable reactive barriers for filtering groundwater contaminated from hydraulic fracturing," *Univ. Ottawa Sci. Undergrad. Res. J.*, vol. 1, p. 55, Aug. 2018.

[32] B. Barnett *et al.*, *Australian groundwater modelling guidelines*. 2012.

[33] M. A. Hossain and D. R. Yonge, "Linear Finite-Element Modeling of Contaminant Transport in Ground Water," *J. Environ. Eng.*, vol. 123, no. 11, pp. 1126–1135, Nov. 1997.

[34] L. Ujfaludi, "Longitudinal dispersion tests in non-uniform porous media," *Hydrol. Sci. J.*, vol. 31, pp. 467–474, 1986.

[35] P. Chaunsali and S. Peethamparan, "Evolution of strength, microstructure and mineralogical composition of a CKD–GGBFS binder," *Cem. Concr. Res.*, vol. 41, no. 2, pp. 197–208, Feb. 2011.

[36] D. N. Ahmed, L. A. Naji, A. A. H. Faisal, N. Al-Ansari, and M. Naushad, "Waste foundry sand/MgFe-layered double hydroxides composite material for efficient removal of Congo red dye from aqueous solution," *Sci. Rep.*, vol. 10, no. 1, p. 2042, Dec. 2020.

[37] K. Wang, S. P. Shah, and A. Mishulovich, "Effects of curing temperature and NaOH addition on hydration and strength development of clinker-free CKD-fly ash binders," *Cem. Concr. Res.*, vol. 34, no. 2, pp. 299–309, Feb. 2004.

[38] R. N. Panda, M. F. Hsieh, R. J. Chung, and T. S. Chin, "FTIR, XRD, SEM and solid state NMR investigations of carbonate-containing hydroxyapatite nano-particles synthesized by hydroxide-gel technique," *J. Phys. Chem. Solids*, vol. 64, no. 2, pp. 193–199, Feb. 2003.

[39] D. N. Ahmed, L. A. Naji, A. A. H. Faisal, N. Al-Ansari, and M. Naushad, "Waste foundry sand/MgFe-layered double hydroxides composite material for efficient removal of Congo red dye from aqueous solution," *Sci. Rep.*, vol. 10, no. 1, p. 2042, Dec. 2020.

[40] A. A. H. Faisal and L. A. Naji, "Simulation of Ammonia Nitrogen Removal from Simulated Wastewater by Sorption onto Waste Foundry Sand Using Artificial Neural Network,"

Assoc. Arab Univ. J. Eng. Sci., vol. 26, no. 1, pp. 28–34, Mar. 2019.

[41] N. Jawad and T. M. Naife, "Mathematical Modeling and Kinetics of Removing Metal Ions from Industrial Wastewater," *Iraqi J. Chem. Pet. Eng.*, vol. 23, no. 4, pp. 59–69, Dec. 2022.

[42] Q. G. Finish and T. M. Naife, "Adsorption Desulfurization of Iraqi Light Naphtha Using Metals Modified Activated Carbon," *J. Eng.*, vol. 27, no. 7, pp. 24 – 41, Jun. 2021.

[43] Q. Chen, D. Yin, S. Zhu, and X. Hu, "Adsorption of cadmium(II) on humic acid coated titanium dioxide," *J. Colloid Interface Sci.*, vol. 367, no. 1, pp. 241–248, Feb. 2012.

[44] P. Liao *et al.*, "Adsorption of tetracycline and chloramphenicol in aqueous solutions by bamboo charcoal: A batch and fixed-bed column study," *Chem. Eng. J.*, vol. 228, pp. 496–505, Jul. 2013.

[45] Z. Aksu and F. Gönen, "Biosorption of phenol by immobilized activated sludge in a continuous packed bed: prediction of breakthrough curves," *Process Biochem.*, vol. 39, no. 5, pp. 599–613, Jan. 2004.

[46] D. C. K. Ko, J. F. Porter, and G. McKay, "Optimised correlations for the fixed-bed adsorption of metal ions on bone char," *Chem. Eng. Sci.*, vol. 55, no. 23, pp. 5819–5829, Dec. 2000.

[47] S. Kundu and A. K. Gupta, "As(III) removal from aqueous medium in fixed bed using iron oxide-coated cement (IOCC): Experimental and modeling studies," *Chem. Eng. J.*, vol. 129, no. 1–3, pp. 123–131, May 2007.

[48] M. H. Marzbali and M. Esmaieli, "Fixed bed adsorption of tetracycline on a mesoporous activated carbon: Experimental study and neuro-fuzzy modeling," *J. Appl. Res. Technol.*, vol. 15, no. 5, pp. 454–463, Oct. 2017.

تحقيق تنقية مياه الجوف الملوثة بمادة الكونغو الحمراء باستخدام حاجز مرشح نافذ بواسطة الحمأة المعدلة من محطات المياه

سداد عادل صالح* طارق محمد نايف **

*،**قسم الهندسة الكيمياوية / كلية الهندسة / جامعة بغداد

*البريد الالكتروني:Sudad.Saleh1607m@coeng.uobaghdad.edu.iq

**البريد الالكتروني:tariq.mohammed@coeng.uobaghdad.edu.iq

الخلاصة

تهدف هذه الدراسة إلى استكشاف إمكانية استخدام الحمأة المستخدمة في محطات المياه (WS) كمادة امتزازية لإزالة صبغة الكونغو الحمراء(CR) ، وهي مادة رخيصة تتولد كنتيجة فرعية لعمليات معالجة المياه. سيتم تحقيق ذلك من خلال ترسيب مركب هيدروكسيد المغنيسيوم والألومنيوم الثنائي الطبقات بحجم نانو على سطح الحمأة. تم تأكيد كفاءة استخدام مركب هيدروكسيد المغنيسيوم والألومنيوم الثنائي الطبقات لتعديل الحمأة المستخدمة في تقنية الحاجز المرشح النافذ من خلال تحليلها باستخدام FTIR و XRD. تم استخدام نموذج إيزوثيرما لانجمير لتوضيح آليات الامتزاز المشاركة في العملية. بالإضافة إلى ذلك، تم استخدام نموذج COMSOL لإنشاء نموذج اختبار مستمر لتحليل نقل الملوثات تحت ظروف متنوعة. أشارت النتائج إلى ترابط قوي، مع معامل تحديد (R2) 0.97 ≤، عند مقارنة توقعات النموذج بالقيم التجريبية، مما يشير إلى دقة النموذج. أظهر نقل المستمر نقاط اختراق أولية سابقة عندما نقل عمق السرير، وتزيد التركيز الأولي ومعدل التدفق .